Three-Dimensional Multihelical Microfluidic Mixers for Rapid Mixing of Liquids

Mohan K. S. Verma, Sambasiva Rao Ganneboyina, Vinayak Rakshith R.,† and Animangsu Ghatak*

Department of Chemical Engineering, Indian Institute of Technology, Kanpur, UP 208016, India

Received September 18, 2007

Rapid mixing of liquids is important for most microfluidic applications. However, mixing is slow in conventional micromixers, because, in the absence of turbulence, mixing here occurs by molecular diffusion. Recent experiments show that mixing can be enhanced by generating transient flow resulting in chaotic advection. While these are planar microchannels, here we show that three-dimensional orientations of fluidic vessels and channels can enhance significantly mixing of liquids. In particular, we present a novel, multihelical microchannel system built in soft gels, for which the helix angle, helix radius, axial length, and even the asymmetry of the channel cross section are easily tailored to achieve the desired mixing. Mixing efficiency increases with helix angle and asymmetry of channel cross section, which leads to orders of magnitude reduction in mixing length over conventional mixers. This new scheme of generating 3D microchannels will help in miniaturization of devices, process intensification, and generation of multifunctional process units for microfluidic applications.

Introduction

Many microfluidic applications require rapid mixing of liquids (e.g., microfluidic total analytical systems,[1,2] DNA sequencing,[3] chemical synthesis,[4,5] process intensification,[6] cell lysis,[7] and transient analysis of intracellular signal transduction processes).[8] Even in nature, the chemical defense system of many insects demands rapid mixing of enzymes and reactants inside glands and fluid vessels for rapid synthesis and discharge of toxic chemicals on predators.[9] However, the small dimension of these fluidic systems is detrimental for mixing as it results in laminar flow inside the channels. In the absence of turbulence, mixing here occurs by the molecular diffusion between different streams. Mixing enhances at low Péclet number ($Pe = Ud/D$, where U is average velocity of flow, d is diameter of the channel, and D is molecular diffusivity) flow, which rather results in the counterintuitive observation that mixing is enhanced at low Reynolds number ($Re = Ud/\upsilon$, where υ is kinematic viscosity). Earlier experiments with channels having grooved walls[10−13] and serpentine or helical structure[5,14−16] have revealed that mixing can be improved by "chaotic advection",[17] which involves breaking, stretching, and folding of liquid streams leading to the increase in interfacial contact between the fluids. While these are examples of microchannels designed in planar platforms, in this article we present novel three-dimensional (3D) microfluidic channel systems that are generated monolithically in poly(dimethylsiloxane) (PDMS) using twisted nylon threads as template.[18] The channels are generated in the form of helices with cross sections consisting of three or more branches, the orientation of which changes along the length of the channel. In contrast to conventional circular and rectangular microchannels, such design leads to inherent asymmetry of the channel cross section, which is altered systematically by varying the number of the branches. We have studied also the effect of helix angle and the mixing length of the microchannel on mixing of two different liquids. These experiments show that the helical mixer facilitates strong chaotic flow even at low Reynolds number, which enhances the mixing efficiency.

Flow of a fluid inside a single curved tube is characterized by the nondimensional Dean's number,[19] which accounts for the

† Current address: Department of chemical engineering, National Institute of Technology, Karnataka, Surathkal, India.

(1) (a) Reyes, D. R.; Iossifidis, D.; Auroux, P.-A.; Manz, A. Micro total analysis systems. I. Introduction, theory, and technology. *Anal. Chem.* **2002**, *74*, 2623−2636. (b) Auroux, P.-A.; Reyes, D. R.; Iossifidis, D.; Manz, A. Micro total analysis systems. II. Analytical standard operations and applications. *Anal. Chem.* **2002**, *74*, 2637−2652.

(2) Beebe, D. J.; Mensing, G. A.; Walker, G. M. Physics and applications of microfluidics in biology. *Annu. Rev. Biomed. Eng.* **2002**, *4*, 261−286.

(3) Burns, M. A.; Johnson, B. N.; Brahmasandra, S. N.; Handique, K.; Webster, J. R.; Krishnan, M.; Sammarco, T. S.; Man, P. M.; Jones, D.; Heldsinger, D.; Mastrangelo, C. H.; Burke, D. T. An integrated nanoliter DNA analysis device. *Science* **1998**, *282*, 484−487.

(4) Losey, M. W.; Schmidt, M. A.; Jensen, K. F. Microfabricated multiphase packed-bed reactors: Characterization of mass transfer and reactions. *Ind. Eng. Chem. Res.* **2001**, *40*, 2555−2562.

(5) Günther, A.; Jhunjhunwala, A. M.; Thalmann, M.; Schmidt, M. A.; Jensen, K. F. Micromixing of miscible liquids in segmented gas-liquid flow. *Langmuir* **2005**, *21*, 1547−1555.

(6) Kreutzer, M. T.; Bakker, J. J. W.; Kapteijn, F.; Moulijn, J. A.; Verheijen, P. J. T. Scaling-up multiphase monolith reactors: Linking residence time distribution and feed maldistribution using isobars. *Ind. Eng. Chem. Res.* **2005**, *44*, 4898−4913.

(7) El-Ali, J.; Gaudet, S.; Günther, A.; Sorger, P. K.; Jensen, K. F. Cell stimulus and lysis in a microfluidic device with segmented gas-liquid flow. *Anal. Chem.* **2005**, *77*, 3629−3636.

(8) Kholodenko, B. N.; Demin, O. V.; Moehren, G.; Hoek, J. B. Quantification of short term signaling by the epidermal growth factor receptor. *J. Biol. Chem.* **1999**, *274*, 30169−30181.

(9) Eisner, T. *For Love of Insects;* Belknap Press of Harvard University Press: Cambridge, MA, 2003.

(10) Stroock, A. D.; Dertinger, S. K.; Ajdari, A.; Mezic, I.; Stone, H. A.; Whitesides, G. M. Chaotic mixer for microchannels. *Science* **2002**, *295*, 647−651.

(11) Stroock, A. D.; Dertinger, S. K.; Whitesides, G. M.; Ajdari, A. Patterning flows using grooved surfaces. *Anal. Chem.* **2002**, *74*, 5306−5312.

(12) Sato, H.; Ito, S.; Tajima, K.; Orimoto, N.; Shoji, S. PDMS microchannels with slanted grooves embedded in three walls to realize efficient spiral flow. *Sens. Actuators, A* **2005**, *119*, 365−371.

(13) Lynn, N. S.; Dandy, D. S. Geometrical optimization of helical flow in grooved micromixers. *Lab on a Chip* **2007**, *7*, 580−587.

(14) Liu, R. H.; Stremler, M. A.; Sharp, K. V.; Olsen, M. G.; Santiago, J. G.; Adrian, R. J.; Aref, H.; Beebe, D. J. Passive mixing in a three-dimensional serpentine microchannel. *J. Microelectromech. Syst.* **2000**, *9*, 190−197.

(15) Park, S. J.; Kim, J. K.; Park, J.; Chung, S.; Chung, C.; Chang, J. K. Rapid three-dimensional passive rotation micromixer using the breakup process. *J. Micromech. Microeng.* **2004**, *14*, 6−14.

(16) Sudarsan, A. P.; Ugaz, M. Multivortex micromixing. *Proc. Natl. Acad. Sci. U.S.A.* **2006**, *103*, 7228−7233.

(17) Aref, H. Stirring by chaotic advection. *J. Fluid Mech.* **1984**, *143*, 1−21.

(18) Verma, M. K. S.; Majumder, A.; Ghatak, A. Embedded template-assisted fabrication of complex microchannels in PDMS and design of a microfluidic adhesive. *Langmuir* **2006**, *22*, 10291−10295.

(19) (a) Dean, W. R. Note on the motion of fluid in a curved pipe. *Philos. Mag.* **1927**, *4*, 208−223. (b) Dean, W. R. The stream-line motion of fluid in a curved pipe. *Philos. Mag.* **1928**, *5*, 673−695.

10.1021/la702895w CCC: $40.75
Published on Web 01/16/2008 PAGE EST: 3.7

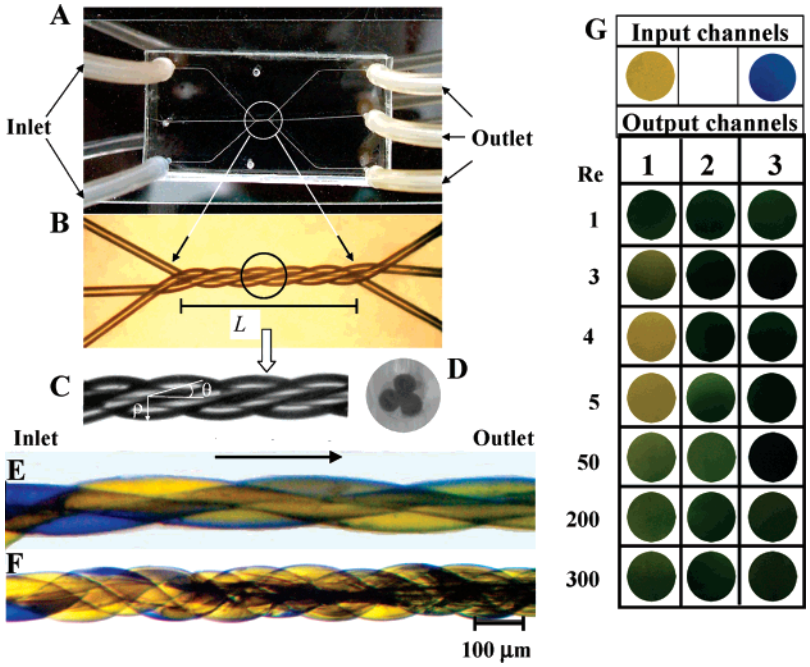

Figure 1. Schematic of mixing experiment in helical microchannels. (A) Triple helical microchannel with controlled mixing length L and the helix angle θ are embedded in a block of PDMS. Two liquid streams colored differently are pumped into the microchannel, and three output samples are taken from outlet ports for image analysis. (B−D) Magnified top and side views of the mixing zone show the geometry of a typical channel. (E, F) Optical images of the side view of microchannels depict progressive mixing of liquids. (E) Obtained for a channel with helix angle $\theta = 12°$ and mixing length $L = 1$ mm at $Re = 1$. (F) $\theta = 36°$, $L = 1$ mm at $Re = 150$. (G) Series of images depict the unmixed color of the input samples and the mixed color of the output samples showing the extent of mixing at various Reynolds numbers inside a microchannel of helix angle $\theta = 15°$ and mixing length $L = 1$ mm.

relative magnitude of inertial and centrifugal to viscous forces: $\kappa = (d/R)^{0.5} Re$; here, R is the radius of curvature of the flow path, d is the diameter of the tube, and Re is the Reynolds number. When the Dean's number is small, the centrifugal force is not strong enough to perturb the axial flow in tube, but for a large enough Dean's number, the axial flow inside the tube is perturbed by a secondary flow in the transverse plane, which can engender chaotic advection in the laminar regime. In the context of mixing of different streams, chaotic flow leads to rapid stretching and overlapping of interfacial area, which enhances the mass transfer. However, for the 2D planar spiral microchannel, the curvilinear path of the fluid is not enough to generate the chaotic advection as it necessitates also time-dependent flow, which is achieved by varying the channel cross section or by the split and recombine arrangement.[14−16] Such requirement of transient flow is not necessary in a 3D microchannel (e.g., in a helical or twisted channel in which the plane of curvature constantly changes so that the planar streamlines of the secondary flow get constantly sheared, giving rise to chaotic trajectories of particles). This effect is further enhanced for the channel systems shown in Figure 1A−C in which the cross section consisting of multiple branches is inherently asymmetric. In such geometry, the strain rate of the cross-sectional flow changes with respect to the angular location, leading to further shearing and distortion of the interfaces. The Reynolds number $Re = Ud/\upsilon$ inside these microchannels is estimated by taking d as the hydraulic diameter: $d = 4A_c/P$, where A_c is the cross-sectional area and P is the wetted perimeter. U and υ are the average fluid velocity inside the channel and fluid kinematic viscosity, respectively. In Figure 1E, we show the optical image of the side view of a microchannel of helix angle $\theta = 12°$ and hydraulic diameter $d = 61$ μm in which two differently colored liquids are pumped in at equal flow rate. At the inlet, we see the presence of two distinctly colored liquids (i.e., yellow and blue) that mix rather slowly at $Re = 1$ via molecular diffusion. As a result, we see incomplete mixing within an axial length of $L = 1$ mm. However, the image in Figure 1F represents a channel in which the helix angle is increased to $\theta = 36°$ while the mixing length is maintained at 1 mm. The progressive mixing of the liquids is very evident here at $Re = 150$, as we see the appearance of convoluted streaks of green color that appear in increasing density toward the outlet. These streaks signify the presence of interface between the lamella structure of two liquid elements that undergo stretching and folding characteristic of the chaotic flows. Interestingly, with continuous feeding of the liquid, such a pattern remains stationary, unlike in turbulent flow in which vortices appear, disappear, and change locations with time. In Figure 1G, we show a series of representative images of the output samples obtained at progressively increasing Reynolds number from a channel of helix angle $\theta = 15°$ and mixing length $L = 1$ mm. From the color of these images, we infer that whereas mixing is nearly complete at low Re ($Re < 3$), it decreases as the flow rate is increased ($3 < Re < 5$). The mixing remains almost unaltered at the intermediate range of $5 < Re < 15$, beyond which mixing increases again because of the chaotic advection triggered by the secondary Dean's flow.

These observations are quantified systematically in Figure 2A, in which we plot the mixing efficiency as a function of the Dean's number for channels of constant mixing length: $L = 1$ mm, hydraulic diameter $d = 61$ μm, and a variety of helix angles: $\theta \approx 6-36°$. Here, the radius of curvature R of the flow path is approximated by considering the radius of curvature of each branch of the helix: $\rho/\sin^2\theta$, where θ is the helix angle and ρ is the helix radius (Figure 1C). Substituting the relation for R, we obtained Dean's number as $\kappa = (d/\rho)^{0.5} Re \sin\theta$. Similar to that of 2D planar spirals, at very low Dean's number, inertial and centrifugal forces are not strong enough to significantly perturb the axial laminar flow so that mixing occurs primarily by the molecular diffusion which is promoted by the long residence time of the liquid in the channel. With increase in

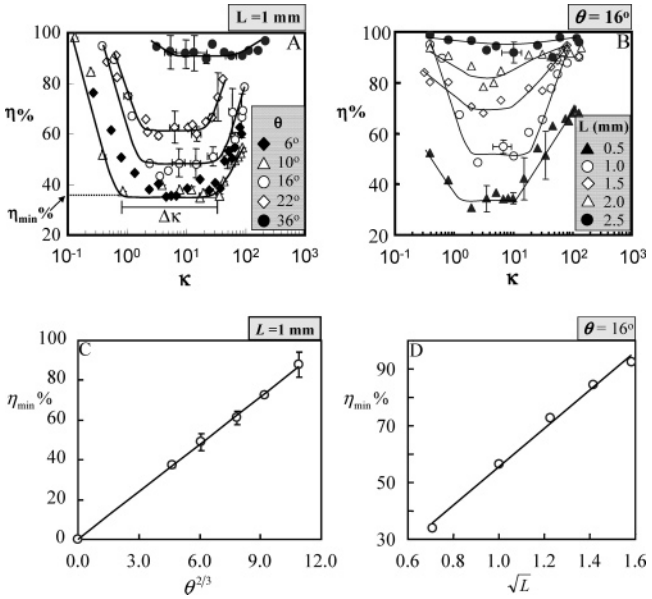

Figure 2. Mixing efficiency as a function of mixing length and helix angle. (A) Mixing efficiency η values obtained from experiments with channels of various helix angles $\theta = 6-36°$ and mixing length $L = 1.0$ mm are plotted with respect to Dean's number κ of the flow of liquid through these channels. (B) Mixing efficiency η values obtained from experiments with channels of various mixing lengths $L = 0.5-2.5$ mm and helix angle $\theta = 16°$ are plotted against Dean's number, κ. The solid lines in these plots are a guide to the eye. (C) Minimum mixing efficiency data η_{min} obtained from graphs in (A) are plotted with respect to the helix angle. The best fit of these data shows that η_{min} increases linearly with $\theta^{2/3}$. (D) Similarly, the best fit of η_{min} obtained from graphs in (B) shows that η_{min} increases linearly with $\sqrt{L}$.

liquid flow rate, however, the reduction in residence time leads to decrease in the mixing efficiency η albeit to different extent for channels of different helix angles: η decreases less for channels of larger helix angle. In contrast to conventional mixers, mixing efficiency does not decrease indefinitely with increase in the liquid flow rate or the Péclet number; two opposing effects arrest the diminishing influence of decrease in the residence time of the liquid: although the axial length L of the channels is kept constant, the effective flow path $L/\cos\theta$ in each helix increases with increase in the helix angle. Furthermore, stronger twisted flow inside the channel triggers the transverse secondary flow, which too becomes significant.[20−23] The combined effects of these two phenomena lead to a critical Dean's number at which the mixing efficiency η reaches a plateau value. The mixing efficiency remains nearly unaltered until a second critical value is reached beyond which η starts to increase again. Thus, the first critical Dean's number is triggered by the in-plane secondary flow, which being inherently asymmetric arrests the fall in the mixing efficiency and maintains it at the plateau value η_{min} until the chaotic advection triggers at a second critical Dean's number $\kappa = 20$. It should be noted, however, that the Dean's number alone cannot capture the fluid flow in such a complicated geometry, as it accounts only for the curvature of the helical tube but does not incorporate the effect of its torsion. In fact, it has been shown by perturbation analysis that the twisting flow in a

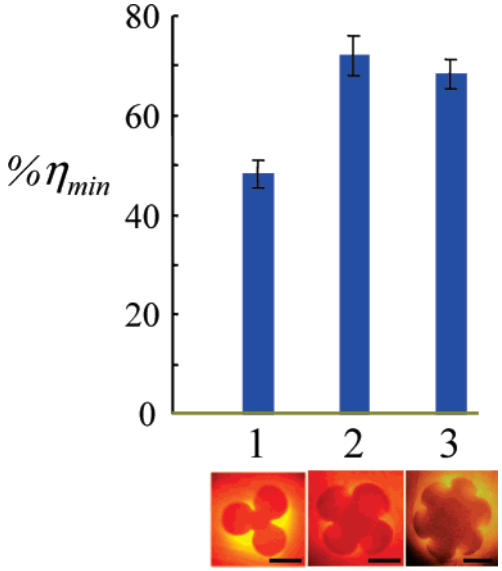

Figure 3. Minimum mixing efficiency for varying shapes of cross sections of the microchannels. Bar chart shows the minimum mixing efficiency in microchannels of mixing length $L = 1.0$ mm, helix angle $\theta = 16°$, and cross sections having three, four, and six cells. The micrographs show the cross section of the microchannels. The scale bar is 50 μm.

single helical tube affects the secondary flow only in the second order of the perturbation expansion of the velocity field.[21,22] As a result, the strength of the radial and the angular components of the velocity that actually affect the transport in the transverse plane depends upon $(\tau d^2/R)^{1/4}$ Re, where the torsion $\tau = \sin\theta \cos\theta/\rho$ and radius of curvature $1/R = \sin^2\theta/\rho$. Thus, the relevant nondimensional number that characterizes the 3D flow in a single helical channel is $Re(d/\rho)^{1/2}\xi$, where $\xi = (\sin^3\theta \cos\theta)^{1/4}$. Indeed, when we plot the data of mixing efficiency η_{min} for channels with various helix angles against ξ, notwithstanding the inherent complicacy of the channel geometry, all data fall on a single straight line (Figure 2C). This signifies that the above scaling deduced for a single helical channel captures well the transverse flow for a triple helical channel. Importantly, in these channels mixing efficiency never decreases below η_{min} corresponding to a given mixing length. For example, Figure 2B shows that, for a microchannel with $\theta = 36°$ and $L = 1.0$ mm, the mixing efficiency exceeds 85% at all values of the Dean's number. Mixing is enhanced further when the mixing length is increased. This is quantified in a different set of experiments in which the mixing length of the microchannels is varied from $L \approx 0.5-2.5$ mm while the helix angle is maintained unaltered at $\theta \approx 16°$ (Figure 2B). The mixing efficiency data plotted in Figure 2D show that η_{min} increases with the mixing length as $\eta_{min} \approx L^{1/2}$, remaining consistently high: $\eta > 90\%$ at all values of κ beyond $L = 2.0$ mm. This result is rationalized by considering that mixing efficiency increases with the extent of transverse diffusion (10): $\eta_{min} \approx (D\tau)^{1/2}$, where $\tau \approx (L/U)$ is the residence time of the liquids inside the microchannel and D is the molecular diffusivity. Substitution of these results yields the scaling relation $\eta_{min} \approx L^{1/2}$ as seen in experiments.

While the discussion above focuses on a triple helical microchannel, we have probed also the effect of asymmetry of the cross section on mixing. We used three, four, and seven twisted nylon threads as templates to prepare channels 1, 2, and 3, respectively, as in Figure 3. The mixing length and the helix angle for all these channels are kept constant ($L = 1.0$ mm and $\theta = 16°$). Mixing experiments were carried out in these channels as shown in Figure 1A. The plateau value of the mixing efficiency

(20) Wang, C. Y. On the low-Reynolds-number flow in a helical pipe. *J. Fluid Mech.* **1981**, *108*, 185−194.
(21) Germano, M. On the effect of torsion on a helical pipe flow. *J. Fluid Mech.* **1982**, *125*, 1−8.
(22) Germano, M.; Oggiano, M. S. Potential flow in helical pipes. *Mechanica* **1987**, *22*, 8−13.
(23) Zhang, J.; Zhang, B. Dean equations extended to a rotating helical pipe flow. *J. Eng. Mech.* **2003**, *129*, 823−829.

from these different experiments is plotted in the bar chart, which shows that the minimum mixing efficiency increases from triple to quadruple helical channel possibly because of increase in level of asymmetry of the cross section. The mixing efficiency decreases thereafter, because with increase in the number of branches in the cross section, its shape asymptotically converges to a symmetric circular one. Thus, maximum efficiency is achieved for an optimum shape of the cross section, which is maximally asymmetric.

To summarize, the method presented here for generating 3D micromixers in PDMS is easily implemented in several other materials (e.g., hydrogel, ceramics, and carbon). The simplicity of this technique allows also modulation of mixing via several controllable parameters (e.g., helix angle, helix radius, and the asymmetry of the channel cross section), which cannot be accomplished in conventional planar systems. Importantly, the mixing efficiency can be maintained at a constant level over a range of values of Reynolds numbers as suggested by the plateau value, which renders the microchannel less susceptible to flow fluctuations and other alterations in the process. While the results presented here concern mixing of two different liquid streams in a triple helical mixer, such a system was effectively used also for mixing of three different liquids. In fact, multihelical microchannels as in Figure 3 can facilitate mixing of multiple different streams. These results signify also that the geometry, particularly the 3D orientations of fluidic vessels, plays an important role in enhancing mixing of liquids in many natural systems. In addition to mixing, such a system should effectively play the role of many other process units (e.g., microreactor, heat exchanger, and separator).

Experimental Section

The microchannels were generated in blocks of cross-linked PDMS (Sylgard 184, Dow Corning product), while slender nylon monofilaments of diameter 50 μm were used to form the 3D oriented template.[18] Solvents such as chloroform and triethylamine were used for swelling the cross-linked PDMS. Food dyes were used for quantifying the extent of mixing inside the channels.

Figure 4 depicts the process of preparing the template for generating the microchannels. Several strands (three to seven) of nylon monofilaments of diameter 50 μm were fixed at equal angular spacing to two parallel rigid cylinders, one of which was rotated relative to the other. The spacing between the disks and the extent of revolution was adjusted to twist the filaments to a desired twisting angle and axial length, which were monitored using a microscope fitted with a camera. The twisted structure was then heated at 100 °C for an hour to form a permanent template that was embedded inside a block of PDMS (Sylgard 184 elastomer). The cross-linked block was immersed in a suitable solvent (e.g., chloroform and triethylamine), which swelled the polymer by 25−30% by length but did not affect the nylon thread. The filaments of the thread were then withdrawn by gently pulling them out of the swollen block, leaving behind a helical channel. The PDMS block was deswollen back by slow evaporation of the solvent. Figure 1a shows the cross section of a typical microchannel which consists of three branches corresponding to a template generated using three monofilaments. The helix angle of these channels was varied between $\theta = 6-36°$, while the mixing length was maintained at $L = 0.5-2.5$ mm. Channels with helix angle $\theta > 36°$ could not be generated because the template could not be maintained axially straight beyond this limit.

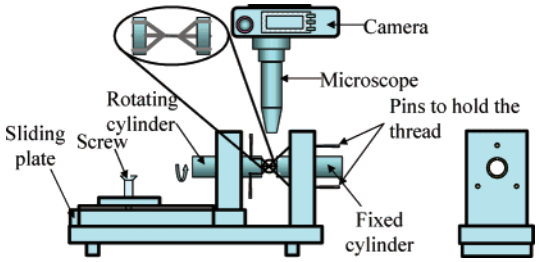

Figure 4. Schematic of a homemade gadget used to generate template for preparing twisted microchannels. Three or more nylon monofilaments are twisted to a desired degree to achieve a particular twisting angle and axial length.

The mixing experiments were done by pumping in these channels two water streams colored differently. Blue and yellow dyes (food colors) were mixed separately with DI water (~10% by weight) and were deaerated in vacuum to remove the dissolved air. The temperature of these liquids was maintained at 22 ± 0.5 °C so as to carry out the experiment at constant viscosity. The two liquid streams were pumped through two inlet ports of a triple helical channel as shown in Figure 1A, while the third unused port was kept closed. The output streams from the mixer were collected separately from the three outlet ports, which were imaged using a digital camera. Mixing efficiency was measured by estimating the gray scale values of the three outlets samples and their standard deviation σ. Similarly, the standard deviation σ_0 of the gray scale values of the pure colors was also obtained. The mixing efficiency was then estimated as $\eta = (1 - \sigma/\sigma_0) \times 100\%$. This definition implies that mixing efficiency is a measure of mass transport between different branches of the mixer.

Acknowledgment. A.G. acknowledges the research initiation grant of IIT Kanpur and the research grant of Department of Science and Technology, India (DST/CHE/20050259) for this work.

LA702895W